SELECTIVE LASER MELTING OF AlCu5MnCdVA: FORMABILITY, MICROSTRUCTURE AND MECHANICAL PROPERTIES

Zhiheng Hu*, Haihong Zhu*, Ting Qi*, Hu Zhang*, Changchun Zhang*, and Xiaoyan Zeng*

*Wuhan National Laboratory for Optoelectronics, Huazhong University of Science and Technology, Wuhan, Hubei, 430074, P. R. of China

Abstract

Selective laser melting (SLM) is an additive manufacture (AM) technique that uses powders to fabricate 3D parts directly. Many researchers are interested in the formability and properties of the established materials manufactured by SLM. The proposed paper illustrates the formability, microstructure and mechanical properties of selective laser melted AlCu5MnCdVA. In this research, crack-free samples with relative density of nearly 100% were produced by SLM from gas atomized powders. Typical columnar crystal and inhomogeneous element distribution were obtained. The mechanical properties were test for the SLMed samples.

Introduction

AlCu5MnCdVA is a high strength cast Al-Cu alloys which has been widely used in aerospace, automobile and military industries [1-3]. However, with the increasing demand of complex structures in these industries, conventional processing techniques can't satisfy the requirements [4]. Thus additive manufacturing (AM) techniques stand out. AM techniques are near-net-shape fabrication techniques to manufacture prototypes or functional products by consolidating successive layers of powders, wires or liquid-based materials [5, 6]. Selective laser melting (SLM) is an AM technique that employs powders melted selectively by a high energy laser beam to manufacture 3D structures directly based on computer aided design (CAD) model [7-9]. It enables rapid fabrication of near full-dense components and offers greatly potential applications for producing complexly shaped parts that cannot be developed by conventional methods [10].

So far, stainless steel [11], nickel alloys [12] and titanium alloys [13] manufactured by SLM have been widely studied. Researchers are also interested in aluminum alloys with the development of SLM because of its high strength to weight ratio. However, the aluminum alloys manufactured by SLM are challenging due to its poor flowability, low absorption and high thermal conductivity [14].

Up to now, researches about aluminum alloys manufactured by SLM have been concentrated on Al-Si alloys. According to the previous papers, AlSi10Mg [15-17], Al-12Si [18],

A356 [19] and A357 [20] have been successfully manufactured by SLM and performed excellent mechanical properties. The high Si-content provides good fluidity and reduces solidification shrinkage. However, only a few works have been devoted to other series of aluminum alloys. Ameli et al. have carried out a comprehensive study of AA 6061 fabricated by SLM [21]. Kaufmann et al. have investigated the influence of process parameters on AW 7075 fabricated by SLM [22]. Wang et al. have studied the microstructure and hardness of the Al-Zn-Mg-Cu manufactured by SLM [23]. Zhang et al. have conducted a detailed research about selective laser melted Al-Cu-Mg alloys [24] and shown the effect of zirconium addition [25]. Very few reports about tensile properties shows that there still are many problems about selective laser melted aluminum alloys whose Si-content is low or 0.

For Al-Cu alloys, they are vulnerable to crack because the addition of Cu makes the crystallization range large [26]. The high crack susceptibility makes it difficult in formability. This work has concentrated on the formability of selective laser melted AlCu5MnCdVA. The microstructure and the mechanical properties have been also investigated.

Materials and experiment procedures

Materials

Gas atomized spherical AlCu5MnCdVA powders with morphology presented in Fig.1 were chosen as the starting materials in this experiment. The range of particle size of the powders was 10-53 μm with an average diameter of 28.7 μm. The particle size was measured using the Malvern UK Mastersizer 3000. The chemical composition of this powder which was measured via ICP-AES (inductive coupled plasma atomic emission spectrometry) is tabulated in Table 1.

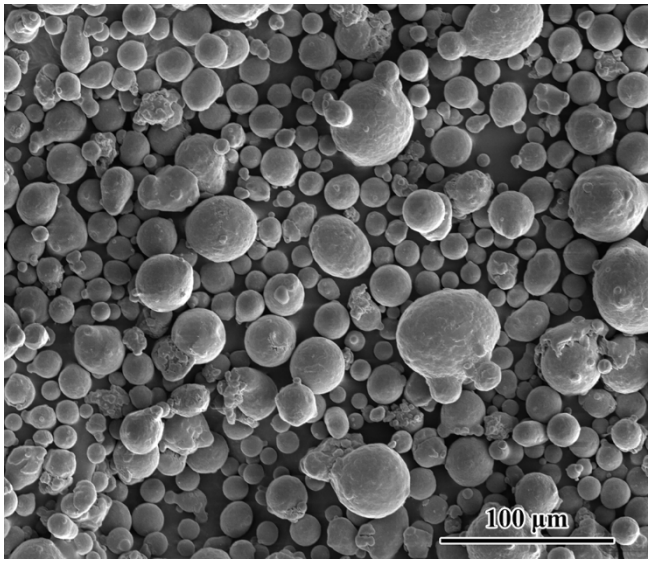

Fig.1 SEM image of starting powders.

Table 1 Chemical composition of AlCu5MnCdVA used in this study.

Elements (Wt/%)	Cu	Fe	Mn	Ti	Zr	V	Cd	Al
AlCu5MnCdVA	5.25	0.04	0.31	0.17	0.086	0.16	0.1	Bal.

SLM process

The experiments were conducted on a self-developed machine (LSNF-1), which consisted of a continuous wave IPG YLR-200 fiber laser (wavelength 1.07μm, maximum laser power 200W), a chamber with atmosphere control and an automatic powder delivery system. More details concerning the SLM system and processing procedure were given in our previous publications [9, 13]. All experiments were carried out under an argon atmosphere with the concentrations of H_2O and O_2 both controlled below 200ppm.

At first, samples with size of 5 mm×5 mm×6 mm were manufactured using different process parameters shown in Table 2 in order to study the relationship between process parameters and relative density. Then one process parameters were chosen to study the microstructure and fabricate the samples for tensile specimens considering the relative density and the machining efficiency. Samples were built vertically which is shown in Fig.2. Then tensile specimens were machined according to the ASTM B557M-10 standard.

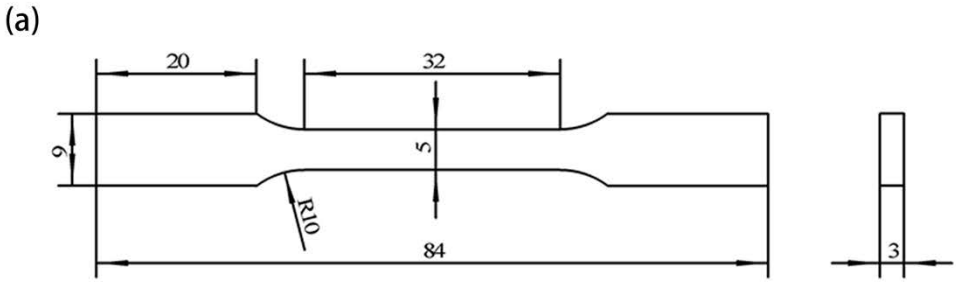

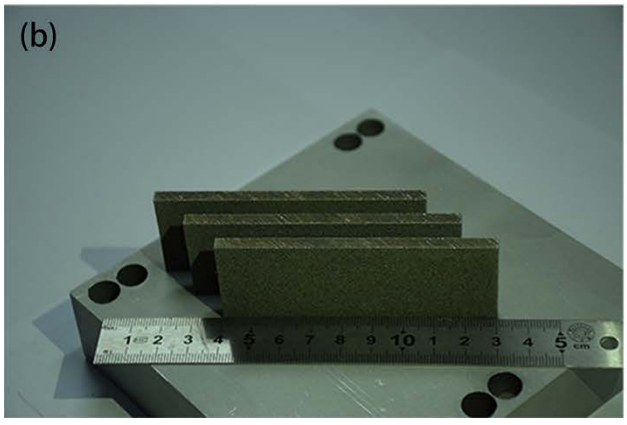

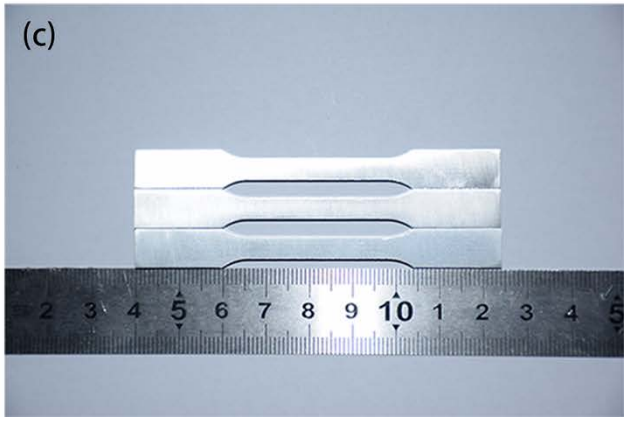

Fig.2 SLMed AlCu5MnCdVA tensile specimens in this study. (a) Configuration; (b) SLM parts; (c) Tensile specimens.

Table 2 SLM process parameters used in the experiments.

Process parameter (Unit)	Value
Laser power (W)	200
Scanning velocity (mm/s)	100, 150, 200, 250, 300, 350
Hatch spacing (μm)	100
Slice thickness (μm)	30
Spot diameter (μm)	115

Characterization

The relative density was evaluated by image processing of four cross-sectional and four vertical-sectional optical micrographs using the Image-Pro Plus 6.0 software after mechanical polishing. Phase identification was performed through an X'Pert-Pro X-ray diffractometer (XRD). For microstructure analysis, samples were etched by a solvent which consists of 2.5 mL HNO3, 1.5 mL HCl, 1 mL HF and 95 mL deionized water. The microstructure was characterized using an optical microscopy (OM, EPIPHOT 300) and the scanning electron microscopy (SEM, FEI Nova NanoSEM 450) equipped with an energy dispersive spectrometry (EDS, Oxford X-Max 50) microprobe system. Tensile tests were carried out using the Zwick/Roell tester at room temperature.

Results and discussions

Formability

Fig.3 shows the effect of laser scanning velocity on the relative density of the SLMed samples. It is observed that the relative density decreases by increasing the scanning velocity. Nearly 100% fully dense samples were achieved when the scanning velocity is low enough. Besides, there is a noticeable loss of density when the scanning velocity increases from 200mm/s to 250mm/s.

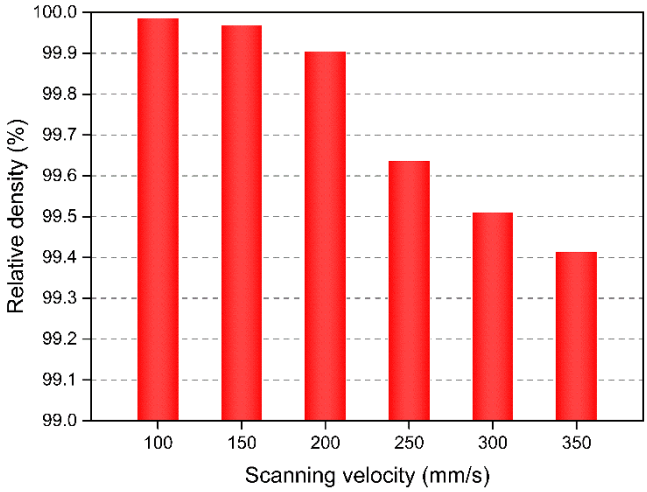

Fig.3 Effect of laser scanning velocity on the relative density.

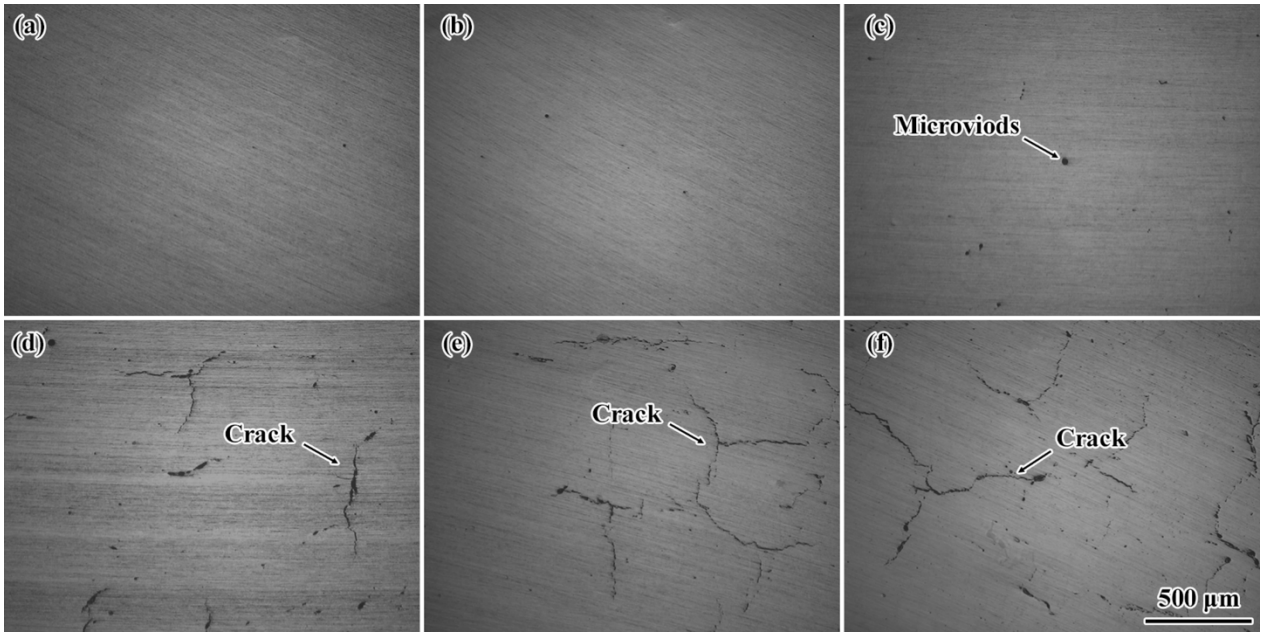

Fig. 4 Microstructures of cross-section obtained at different scanning velocity: (a) 100 mm/s; (2) 150 mm/s; (c) 200 mm/s; (d) 250 mm/s; (e) 300 mm/s; (f) 350 mm/s.

Fig.4 demonstrates the microstructures of cross-section obtained at different scanning velocity. It confirms the inverse relationship between the scanning velocity and the relative density shown in Fig.3. At a lower scanning velocity, there are nearly no defects observed. A lower scanning velocity can make the temperature of the molten pool higher, thus the bubble produced during melting can escape from the molten pool because of the lower liquid viscosity [9]. At the same time, there is sufficient liquid reflux time during the solidification so that the crack can be prevented. As the scanning velocity increases, the microvoids increase due to the

decrease of the temperature of the molten pool. As the scanning velocity increases further, solidification cracks were observed. What's more, the crack density increases with the increase of the scanning velocity. Combining with Fig.3, it is obvious that the noticeable loss of density is due to the appearance of crack. All of these confirm that the formability of the SLMed AlCu5MnCdVA is strongly dependent on scanning velocity.

Microstructure

Taking the machining efficiency into account, the samples fabricated using 150 mm/s is selected as the detailed study objects. XRD patterns of the powder and SLMed samples are shown in Fig.5. It can be seen that Al_2Cu was detected at the powder and the SLMed samples. It is quite different from the SLMed Al-Cu-Mg which is published before [24]. Because of the absence of Mg, the Cu element either precipitates in Al_2Cu or remains in Al-matrix supersaturated solid solution. At the same time, the percentage in weight of Cu is greater. Therefore, it is easier for Al_2Cu to form. The increased content exceeds the XRD limitation in detecting low volume concentrations so Al_2Cu has been detected.

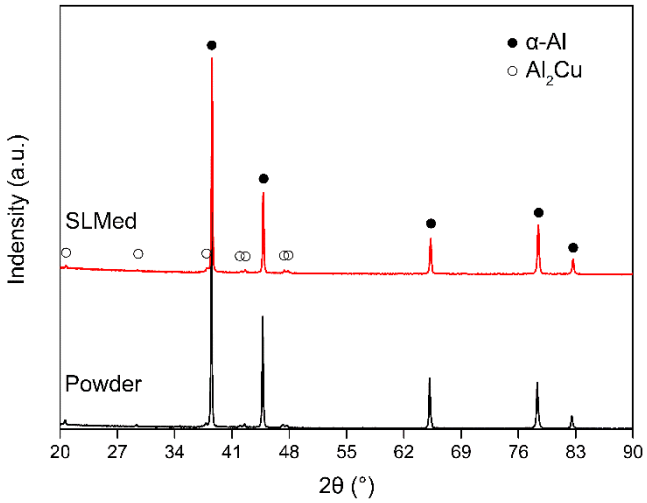

Fig.5 XRD pattern of the powder and SLMed samples.

Fig.6 shows the optical micrographs of the SLMed sample fabricated at laser scanning velocity of 150 mm/s. In Fig.6a, the molten pools with cylindrical shape have been observed and they are closely stacked to exhibit a good metallurgical bonding between the tracks. In addition, typical columnar crystals have been observed and they grew epitaxially along the building direction. In Fig.6b, the columnar grain boundaries are more obvious. The direction of the boundaries changes as the layer changes, which indicates the growth of columnar crystals is influenced by the scanning direction. At the same time, it can be seen that there are dendrites at the molten pool boundaries. They grew along the direction which points to the center of the molten pool. Fig.6c and Fig.6d is the microstructure of the cross section. Fig.6c shows the laser tracks corresponding to the raster scanning with 90° phase angle between the layers. Fig.6d

shows columnar grain boundaries at the cross section which corresponding to the Fig.6b. At the same time, there is some enrichment at the molten pool boundaries.

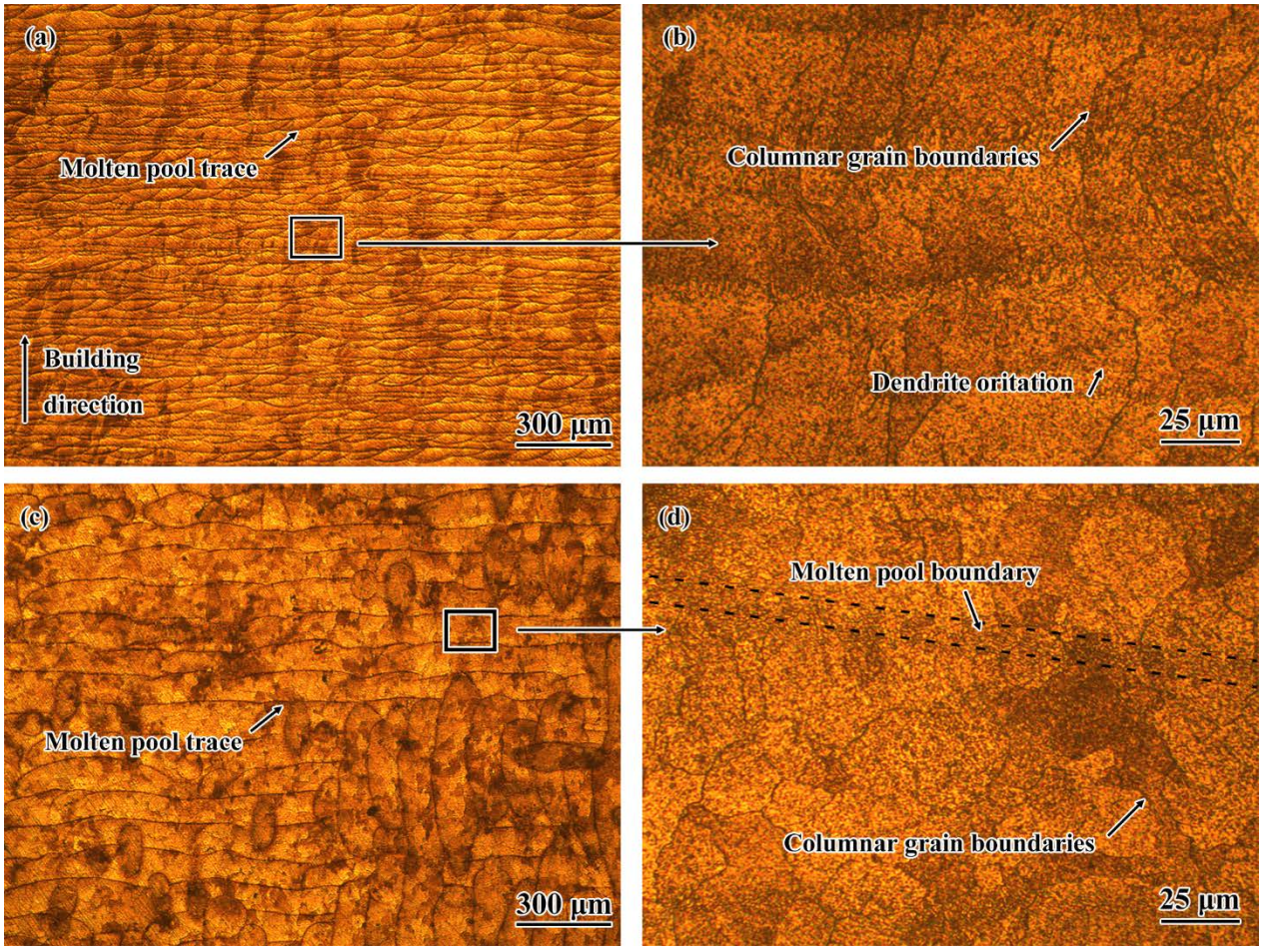

Fig.6 optical micrographs of SLMed sample fabricated at laser scanning velocity of 150 mm/s: (a) vertical section; (b) details shown in (a); (c) cross section; (d) details shown in (c).

Fig.7 shows the results of the element mapping. From the SEM image, it can be seen that the microstructure consists of the white precipitate and the gray α-Al matrix. According to the distribution of Cu elements and the XRD results, it can be drawn that the white precipitate is Al_2Cu. In addition, it can be observed that Al_2Cu exists in three form: one is freely granular in the molten pool, one is dendritic at the molten pool boundaries and one is linked to be filiform at the columnar grain boundaries. The dendritic precipitate at the molten pool boundaries also represents there is substantial grain-growth at the interface region because of the remelting at the interface region [24]. The filiform precipitate indicates there is stable temperature gradient along the columnar grain boundaries. In Fig.7, the Cu elements were inhomogeneous distributed on the vertical direction, indicating that there is element segregation in this SLM process. The Cu elements preferred to gather at the molten pool boundaries and the columnar grain boundaries.

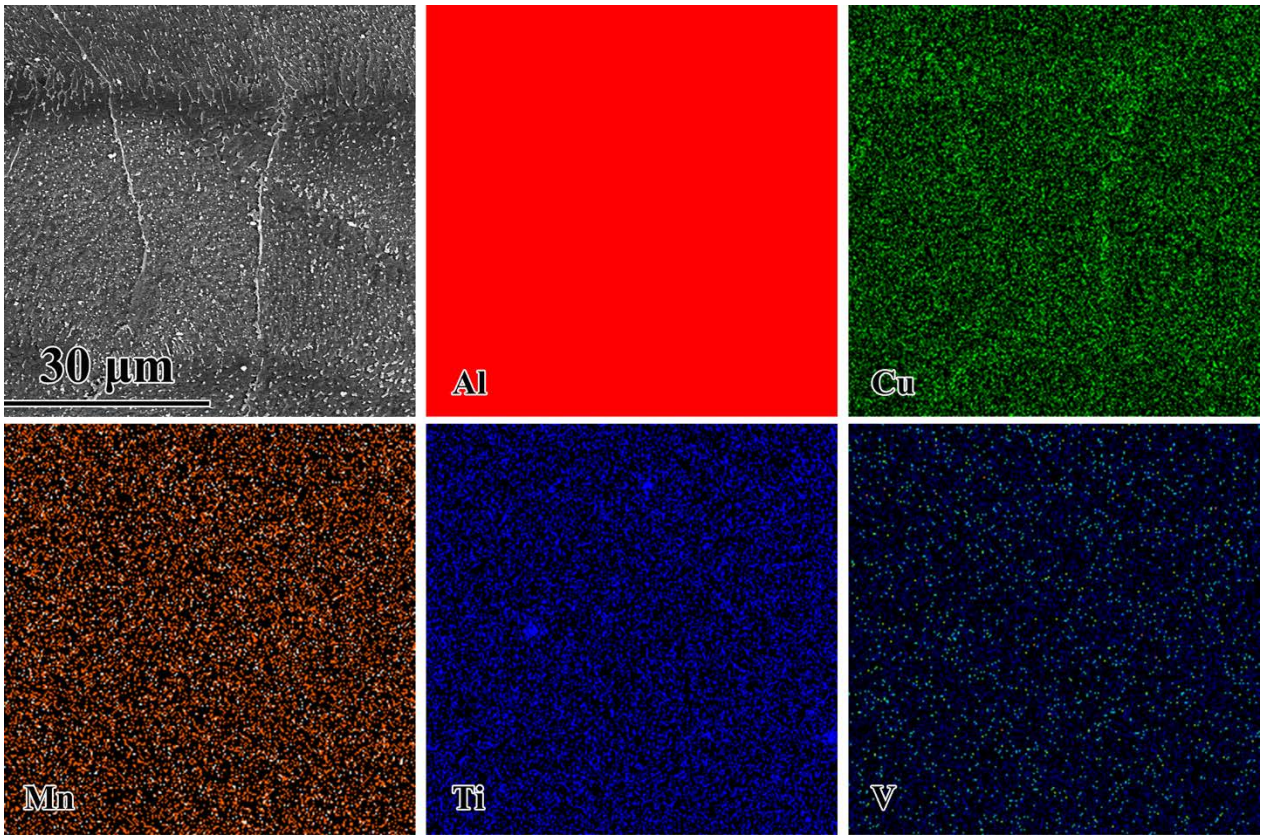

Fig.7 EDS map of individual elements in dense SLMed AlCu5MnCdVA sample.

Mechanical properties

Table 3 shows the tensile properties of the specimens. The as-fabricated specimens shows a not good mechanical properties: the average value of the yield strength is 159.030 MPa, the average value of the ultimate tensile strength is 286.105 MPa and the average value of the elongation is 5.92%. As AlCu5MnCdVA is a heat-treatable aluminum alloys, there are many trace strengthening phase after proper heat treatment. They are absent or little in the as-fabricated samples, which leads to a poor mechanical properties.

Table 3 Tensile properties of the SLM samples.

State	σ0.2/MPa	UTS/MPa	ε/%
As-fabricated AlCu5MnCdVA	150.01-164.041	282.963-291.635	5.58-6.47

Conclusions

In this study, AlCu5MnCdVA and tensile specimens have been successfully fabricated by SLM. Following conclusions can be drawn:

1. AlCu5MnCdVA fabricated by SLM with high relative density of nearly 100% can be obtained. Scanning velocity plays an important role in SLM process. The relatively low scanning velocity can prevent the microviods and the crack. The high scanning velocity will lead to the formation of the crack.

2. The typical columnar crystals formed after SLM process. The phases consist of α-Al and Al_2Cu. There are Cu elements segregation in this SLM process. The Cu prefers to gather at the molten pool boundaries and the columnar grain boundaries.

3. The tensile tests were conducted. The as-fabricated specimens shows a not good mechanical properties. As AlCu5MnCdVA is a heat-treatable aluminum alloys, suitable heat treatment should be conducted to improve the mechanical properties.

Future works

As that the suitable heat treatment is necessary for the SLMed samples is proposed. The future works may concentrate on the influence of the heat treatment on the SLMed AlCu5MnCdVA.

Acknowledgements

This research is supported by the National Natural Science Foundation of China (61475056) and the National Program on Key Basic Research Project of China (613281). The authors would like to thank the Analytical and Testing Center of HUST. Special thanks for Mr. Wu's SEM operating.

References

[1] W. Wang, G. Wang, Y. Hu, G. Guo, T. Zhou, Y.Rong, *Temperature-dependent constitutive behavior with consideration of microstructure evolution for as-quenched Al-Cu-Mn alloy*. Materials Science and Engineering A, 2016. 678: p. 85-92.
[2] B. Li, Y. Shen, W. Hu, *Casting defects induced fatigue damage in aircraft frames of ZL205A aluminum alloy – A failure analysis.* Materials and Design, 2011. 32: p.2570-2582.
[3] Y. Wang, S. Wu, X. Xue, R. Chen, J. Zhang, W. Xiao, *Formation mechanism and criterion of inear segregation in ZL205A alloy*. Transactions of Nonferrous Metals Society of China, 2014. 24: p.3632-3638.
[4] T. B. Sercombe, G. B. Schaffer, *Rapid Manufacturing of Aluminum Components.* Science, 2003. 301: p. 1225-1227.

[5] D. K. Do, P. Li, *The effect of laser energy input on the microstructure, physical and mechanical properties of Ti-6Al-4V alloys by selective laser melting.* Virtual and Physical Prototyping, 2016. 11(1): p.41-47.
[6] J. Yang, H. Yang, H. Yu, Z. Wang, X. Zeng, *Corrosion Behavior of Additive Manufactured Ti-6Al-4V Alloy in NaCl Solution.* Metallurgical and Materials Transactions A, 2017. p.1-11.
[7] C. Weingarten, D. Buchbinder, N. Pirch, W. Meiners, K. Wissenbach, R. Poprawe, *Formation and reduction of hydrogen porosity during selective laser melting of AlSi10Mg.* Journal of Materials Processing Technology, 2015. 221: p.112-120.
[8] J. Vaithilingam, S. Kilsby, R. D. Goodridge, S. D. R. Christie, S. Edmondson, R. J. M. Hague, *Immobilisation of an antibacterial drug to Ti6Al4V components fabricated using selective laser melting.* Applied Surface Science, 2014. 314: p.642-654.
[9] Z. Hu, H. Zhu, H. Zhang, X. Zeng, *Experimental investigation on selective laser melting of 17-4PH stainless steel.* Optics & Laser Technology, 2017. 87: p.17-25.
[10] S. Bremen, W. Meiners, A. Diatlov, *Selective Laser Melting.* Laser Technik Journal, 2012. 9(2): p.33-38.
[11] H. Gu, H. Gong, D. Pal, K. Rafi, T. Starr, B. Stucker, *Influences of energy density on porosity and microstructure of selective laser melted 17-4PH stainless steel.* Solid Freeform Fabrication Symposium Proceedings. Austin, TX: University of Texas, 2013.
[12] K. N. Amato, S. M. Gaytan, L. E. Murr, E. Martinez, P. W. Shindo, J. Hernandez, S. Collins, F. Medina, *Microstructures and mechanical behavior of Inconel 718 fabricated by selective laser melting.* Acta Materialia, 2012. 60(5): p.2229-2239.
[13] K. Wei, Z. Wang, X. Zeng, *Preliminary investigation on selective laser melting of Ti-5Al-2.5Sn α-Ti alloy: From single tracks to bulk 3D components.* Journal of Materials Processing Technology, 2017. 244: p. 73-85.
[14] E. Louvis, P. Fox, C. J. Sutcliffe, *Selective laser melting of aluminium components.* Journal of Materials Processing Technology, 2011. 211(2): p.275-284.
[15] L. P. Lam, D. Q. Zhang, Z. H. Liu, *Phase analysis and microstructure characterisation of AlSi10Mg parts produced by Selective Laser Melting.* Virtual and Physical Prototyping, 2015. 10(4): p.207-215.
[16] U. Tradowsky, J. White, R. M. Ward, N. Read, W. Reimers, M. M. Attallah, *Selective laser melting of AlSi10Mg: Influence of post-processing on the microstructural and tensile properties development.* Materials and Design, 2016. 105: p.212-222.
[17] W. Li, S. Li, J. Liu, A. Zhang, Y. Zhou, Q. Wei, C. Yan, Y. Shi, *Effect of heat treatment on AlSi10Mg alloy fabricated by selective laser melting: Microstructure evolution, mechanical properties and fracture mechanism.* Materials Science and Engineering A, 2016. 663: p.116-125.
[18] K. G. Prashanth, S. Scudino, H. J. Klauss, K. B. Surreddi, L. Löber, Z. Wang, A. K. Chaubey, U. Kühn, J. Eckert. *Microstructure and mechanical properties of Al–12Si produced by selective laser melting: Effect of heat treatment.* Materials Science and Engineering A, 2014. 590: p.153-160.

[19] T. Kimura, T. Nakamoto, *Microstructures and mechanical properties of A356 (AlSi7Mg0.3) aluminum alloy fabricated by selective laser melting.* Materials and Design, 2016. 89: p.1294-1301.
[20] H. Rao, S. Giet, K. Yang, X. Wu, C. H. J. Davies, The influence of processing parameters on aluminium alloy A357 manufactured by Selective Laser Melting. Materials and Design, 2016. 109: p.334-346.
[21] M. Ameli, B. Agnew, P.S. Leung, B. Ng, C. J. Sutcliffe, J. Singh, R. McGlen, *A novel method for manufacturing sintered aluminium heat pipes (SAHP).* Applied Thermal Engineering, 2013. 52(2): p.498-504.
[22] N. Kaufmann. M. Imran. T.M. Wischeropp. C. Emmelmann. S. Siddique. F. Walther. *Influence of Process Parameters on the Quality of Aluminium Alloy EN AW 7075 Using Selective Laser Melting (SLM).* Physics Procedia, 2016. 83: p.918-926.
[23] P. Wang, H. C. Li, K. G. Prashanth, J. Eckert, S. Scudino, *Selective laser melting of Al-Zn-Mg-Cu: Heat treatment, microstructure and mechanical properties.* Journal of Alloys and Compounds, 2017. 707: p.287-290.
[24] H. Zhang, H. Zhu, T. Qi, Z. Hu, X. Zeng. Selective laser melting of high strength Al–Cu–Mg alloys: processing, microstructure and mechanical properties. Materials Science and Engineering A, 2016. 656: p.47-54.
[25] H. Zhang, H. Zhu, X. Nie, J. Yin, Z. Hu, X. Zeng. Effect of Zirconium addition on crack, microstructure and mechanical behavior of selective laser melted Al-Cu-Mg alloy. Scripta Materialia, 2017. 134: p.6-10.
[26] Z. Yang, A. Wang, Z. Weng, D. Xiong, B. Ye, X. Qi, *Porosity elimination and heat treatment of diode laser-clad homogeneous coating on cast aluminum-copper alloy.* Surface and Coatings Technology, 2017. 321: p.26-35.